Statistics of the two-point transmission at Anderson localization transitions

Cécile Monthus and Thomas Garel
Institut de Physique Théorique, CNRS and CEA, Saclay, 91191 Gif-sur-Yvette Cedex, France
(Received 12 March 2009; revised manuscript received 4 May 2009; published 27 May 2009)

At Anderson critical points, the statistics of the two-point transmission T_L for disordered samples of linear size L is expected to be multifractal with the following properties [Janssen *et al.*, Phys. Rev. B **59**, 15836 (1999)]: (i) the probability to have $T_L \sim 1/L^{\kappa}$ behaves as $L^{\Phi(\kappa)}$, where the multifractal spectrum $\Phi(\kappa)$ terminates at $\kappa=0$ as a consequence of the physical bound $T_L \leq 1$; (ii) the exponents $X(q)$ that govern the moments $\overline{T_L^q} \sim 1/L^{X(q)}$ become frozen above some threshold: $X(q \geq q_{\rm sat})=-\Phi(\kappa=0)$, i.e., all moments of order $q \geq q_{\rm sat}$ are governed by the measure of the rare samples having a finite transmission ($\kappa=0$). In the present paper, we test numerically these predictions for the ensemble of $L \times L$ power-law random-banded matrices, where the random hopping $H_{i,j}$ decays as a power law $(b/|i-j|)^a$. This model is known to present an Anderson transition at $a=1$ between localized ($a>1$) and extended ($a<1$) states with critical properties that depend continuously on the parameter b. Our numerical results for the multifractal spectra $\Phi_b(\kappa)$ for various b are in agreement with the relation $\Phi(\kappa \geq 0)=2[f(\alpha=d+\frac{\kappa}{2})-d]$ in terms of the singularity spectrum $f(\alpha)$ of individual critical eigenfunctions, in particular the typical exponents are related via the relation $\kappa_{\rm typ}(b)=2[\alpha_{\rm typ}(b)-d]$. We also discuss the statistics of the two-point transmission in the delocalized phase and in the localized phase.

DOI: 10.1103/PhysRevB.79.205120 PACS number(s): 71.30.+h, 71.23.An, 72.15.Rn, 05.45.Df

I. INTRODUCTION

Since its discovery 50 years ago,[1] Anderson localization has remained a very active field of research (see the reviews in Refs. 2–8). One of the most important property of Anderson localization transitions is that critical eigenfunctions are described by a multifractal spectrum $f(\alpha)$ defined as follows (for more details see for instance the reviews in Refs. 6 and 8): in a sample of size L^d, the number $\mathcal{N}_L(\alpha)$ of points $\vec{r}$, where the weight $|\psi(\vec{r})|^2$ scales as $L^{-\alpha}$ behaves as

$$\mathcal{N}_L(\alpha) \underset{L\to\infty}{\propto} L^{f(\alpha)}. \tag{1}$$

The inverse participation ratios (IPRs) can be then rewritten as an integral over α,

$$Y_q(L) \equiv \int_{L^d} d^d\vec{r} |\psi(\vec{r})|^{2q} \simeq \int d\alpha L^{f(\alpha)} L^{-q\alpha} \underset{L\to\infty}{\simeq} L^{-\tau(q)}. \tag{2}$$

The exponent $\tau(q)$ can be obtained via a saddle-point calculation in α, and one obtains the Legendre transform formula[6,8]

$$q = f'(\alpha),$$

$$\tau(q) = q\alpha - f(\alpha). \tag{3}$$

These scaling behaviors, which concern individual eigenstates ψ, can be translated for the local density of states,

$$\rho_L(E,\vec{r}) = \sum_n \delta(E-E_n)|\psi_{E_n}(\vec{r})|^2, \tag{4}$$

as follows: for large L, when the L^d energy levels become dense, the sum of Eq. (4) scales as

$$\rho_L(E,\vec{r}) \propto L^d |\psi_E(\vec{r})|^2 \tag{5}$$

and its moments involve the exponents $\tau(q)$ introduced in Eq. (2)

$$\overline{[\rho_L(E,\vec{r})]^q} \underset{L\to\infty}{\propto} \frac{1}{L^{\Delta(q)}}, \quad \text{with } \Delta(q) = \tau(q) - d(q-1). \tag{6}$$

These notions concern one-point functions, and it is natural to consider also the statistics of two-point functions. In particular, a very interesting observable to characterize Anderson transitions is the two-point transmission T_L when the disordered sample of size L^d is attached to one incoming wire and one outcoming wire:[9,10] (i) it remains finite in the thermodynamic limit only in the delocalized phase so that it represents an appropriate order parameter for the conducting/nonconducting transition; (ii) exactly at criticality, it displays multifractal properties in direct correspondence with the multifractality of critical eigenstates, i.e., it displays strong fluctuations that are not captured by more global definitions of conductance. More precisely, as first discussed in Ref. 9 for the special case of the two-dimensional quantum-Hall transition, the critical probability distribution of the two-point transmission T_L takes the form

$$\text{Prob}(T_L \sim L^{-\kappa}) dT \underset{L\to\infty}{\propto} L^{\Phi(\kappa)} d\kappa, \tag{7}$$

and its moments involve nontrivial exponents $X(q)$

$$\overline{T_L^q} \sim \int d\kappa L^{\Phi(\kappa)-q\kappa} \underset{L\to\infty}{\propto} L^{-X(q)}. \tag{8}$$

As stressed in Ref. 9 the physical bound $T_L \leq 1$ on the transmission implies that the multifractal spectrum exists only for $\kappa \geq 0$, and this termination at $\kappa=0$ leads to a complete freezing of the moments exponents

$$X(q) = X(q_{\rm sat}) \quad \text{for} \quad q \geq q_{\rm sat} \tag{9}$$

at the value $q_{\rm sat}$ where the saddle point of the integral of Eq. (8) vanishes $\kappa(q \geq q_{\rm sat})=0$. It is very natural to expect some relation between the two multifractal spectra $f(\alpha)$ and $\Phi(\kappa)$, and the possibility proposed in Ref. 9 is that before the freezing of Eq. (9) occurs, the transmission should scale as the

product of two independent local densities of states [Eq. (6)]

$$X(q) = 2\Delta(q) \quad \text{for} \quad q \leq q_{\text{sat}}. \tag{10}$$

We refer to Ref. 9 for physical arguments in favor of this relation. Eqs. (9) and (10) for the moments exponents are equivalent to following relation between the two multifractal spectra

$$\Phi(\kappa \geq 0) = 2\left[f\left(\alpha = d + \frac{\kappa}{2} \right) - d \right]. \tag{11}$$

In this paper, our aim is to test numerically these predictions for the statistics of the two-point transmission T_L at the critical points of the power-law random-banded matrix (PRBM) model, where one parameter allows us to interpolate continuously between weak multifractality and strong multifractality. We will also discuss the statistics of the two-point transmission off criticality.

The paper is organized as follows. In Sec. II, we introduce the PRBM model and the scattering geometry used to define the two-point transmission. In Sec. III, we present our numerical results concerning the multifractal statistics of the two-point transmission at criticality. We then discuss the statistics of the two-point transmission in the localized phase (Sec. IV) and in the delocalized phase (Sec. V), respectively. Our conclusions are summarized in Sec. VI. Appendices A and B contain more details on the numerical computations.

II. MODEL AND OBSERVABLES

Beside the usual short-range Anderson tight-binding model in finite dimension d, other models displaying Anderson localization have been studied, in particular, the PRBM model, which can be viewed as a one-dimensional model with long-ranged random hopping decaying as a power law $(b/r)^a$ of the distance r with exponent a and parameter b (see below for a more precise definition of the model). The Anderson transition at $a=1$ between localized $(a>1)$ and extended $(a<1)$ states has been characterized in Ref. 11 via a mapping onto a nonlinear sigma model. The properties of the critical points at $a=1$ have been then much studied, in particular, the statistics of eigenvalues[12–14] and the multifractality of eigenfunctions,[15–20] including boundary multifractality.[21] The statistics of scattering phases, Wigner delay times, and resonance widths in the presence of one external wire have been discussed in Refs. 22 and 23. Related studies concern dynamical aspects,[24] the case with no on-site energies,[25] and the case of power-law hopping terms in dimension $d>1$.[26–28] In this paper, we consider the PRBM in a ring geometry (dimension $d=1$ with periodic boundary conditions) in the presence of two external wires to measure the transmission properties.

A. Power-law random-banded matrices with periodic boundary conditions

We consider L sites $i=1,2,\ldots,L$ in a ring geometry with periodic boundary conditions, where the appropriate distance $r_{i,j}$ between the sites i and j is defined as[15]

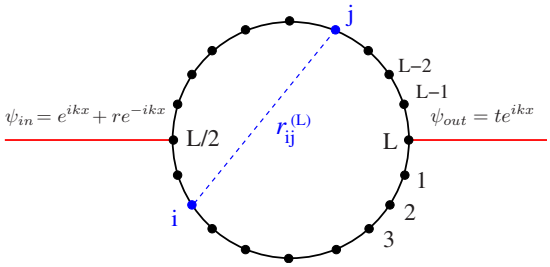

FIG. 1. (Color online) The ensemble of power-law random-banded matrices of size $L \times L$ can be represented as a ring of L sites, where the matrix element $H_{i,j}$ between the sites i and j is a Gaussian variable of zero mean $\overline{H_{i,j}}=0$ and of variance given by Eq. (13) in terms of the distance $r_{i,j}$ of Eq. (12). In this paper, we study the statistics of the Landauer transmission $T_L=|t|^2$ when an incoming wire is attached at the site $L/2$ and an outgoing wire is attached at the site L (see text for more details).

$$r_{i,j}^{(L)} = \frac{L}{\pi} \sin\left(\frac{\pi(i-j)}{L} \right). \tag{12}$$

The ensemble of power-law random-banded matrices of size $L \times L$ is then defined as follows: the matrix elements $H_{i,j}$ are independent Gaussian variables of zero mean $\overline{H_{i,j}}=0$ and of variance

$$\overline{H_{i,j}^2} = \frac{1}{1 + \left(\frac{r_{i,j}}{b} \right)^{2a}}. \tag{13}$$

The most important properties of this model are the following. The value of the exponent a determines the localization properties:[11] for $a>1$ states are localized with integrable power-law tails, whereas for $a<1$ states are delocalized. At criticality $a=1$, states become multifractal[15–18] and exponents depend continuously on the parameter b, which plays a role analog to the dimension d in short-range Anderson transitions:[15] the limit $b \gg 1$ corresponds to weak multifractality (analogous to the case $d=2+\epsilon$) and can be studied via the mapping onto a nonlinear sigma model,[11] whereas the case $b \ll 1$ corresponds to strong multifractality (analogous to the case of high dimension d) and can be studied via Levitov renormalization.[15,29] Other values of b have been studied numerically.[15–18]

B. Scattering geometry used to define to two-point transmission

In quantum coherent problems, the most appropriate characterization of transport properties consists in defining a scattering problem where the disordered sample is linked to incoming wires and outgoing wires and in studying the reflection and transmission coefficients. This scattering theory definition of transport, first introduced by Landauer,[30] has been often used for one-dimensional systems[31–33] and has been generalized to higher dimensionalities and multiprobe measurements (see the review in Ref. 34). In the present paper, we focus on the Landauer transmission for the scattering problem shown on Fig. 1: an incoming wire is attached at the site $L/2$ and an outgoing wire is attached at the

site L. We are thus interested into the eigenstate $|\psi\rangle$ that satisfies the Schrödinger equation,

$$H|\psi\rangle = E|\psi\rangle, \tag{14}$$

inside the disorder sample characterized by the random $H_{i,j}$ and in the perfect wires characterized by no on-site energy and by hopping unity between nearest neighbors. Within these perfect wires, one requires the plane-wave forms

$$\psi_{\text{in}}(x \leq x_{L/2}) = e^{ik(x-x_{L/2})} + re^{-ik(x-x_{L/2})},$$

$$\psi_{\text{out}}(x \geq x_L) = te^{ik(x-x_L)} \tag{15}$$

These boundary conditions define the reflection amplitude r of the incoming wire and the transmission amplitude t of the outgoing wire. The Landauer transmission

$$T \equiv |t|^2 = 1 - |r|^2 \tag{16}$$

is then a number in the interval $[0,1]$. More details on the numerical computation of the transmission in a given sample are given in Appendix A.

To satisfy the Schrödinger Equation of Eq. (14) within the wires with the forms of Eq. (15), one has the following relation between the energy E and the wave vector k:

$$E = 2\cos k. \tag{17}$$

To simplify the discussion, we will focus in this paper on the case of zero energy $E=0$ (wave vector $k=\pi/2$) that corresponds to the center of the band.

In the following, we study numerically the statistical properties of the Landauer transmission T for rings of size $50 \leq L \leq 1800$ with corresponding statistics of $10 \times 10^8 \geq n_s(L) \geq 2400$ independent samples. For typical values, the number $n_s(L)$ of samples is sufficient even for the bigger sizes, whereas for the measure of multifractal spectrum, we have used only the smaller sizes where the statistics of samples was sufficient to measure correctly the rare events.

III. STATISTICS OF THE TWO-POINT TRANSMISSION AT CRITICALITY ($a=1$)

As recalled in Sec. I, the two-point transmission T_L is expected to display multifractal statistics at criticality.[9] We first focus on the scaling of the typical transmission before we turn to the multifractal spectrum and the moments of arbitrary order.

A. Typical transmission at criticality ($a=1$)

As discussed in Refs. 9 and 10, the typical transmission

$$T_L^{\text{typ}} \equiv e^{\overline{\ln T_L}} \tag{18}$$

is expected to decay at criticality with some power law

$$T_L^{\text{typ}} \underset{L\to\infty}{\propto} \frac{1}{L^{\kappa_{\text{typ}}}}, \tag{19}$$

where the exponent κ_{typ} is directly related via the relation

$$\kappa_{\text{typ}} = 2(\alpha_{\text{typ}} - d) \tag{20}$$

to the typical exponent α_{typ} that characterizes the typical weight of eigenfunctions

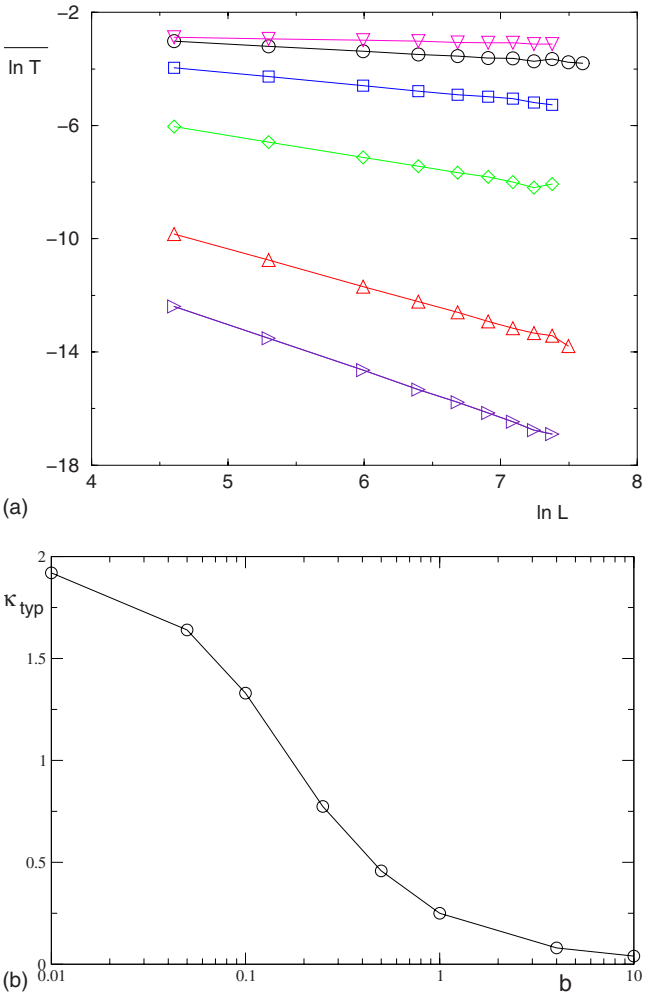

FIG. 2. (Color online) Scaling of the typical transmission T_L^{typ} at criticality $a=1$ for various values of the parameter b: (a) $\ln T_L^{\text{typ}} \equiv \overline{\ln T_L}$ as a function of $\ln L$ for various values of $b=4$ (▽), 1 (○), 0.5 (□), 0.25 (◇), 0.1 (△), and 0.05 (▷) (the two other values $b=10$ and $b=0.01$ we have studied are not shown here for clarity): the slope yields the typical exponent $\kappa_{\text{typ}}(b)$ of Eq. (22). (b) critical exponent $\kappa_{\text{typ}}(b)$ as a function of b.

$$|\psi(\vec{r})|^2_{\text{typ}} \propto \frac{1}{L^{\alpha_{\text{typ}}}}. \tag{21}$$

This typical value α_{typ} corresponds to the maximum value $f(\alpha_{\text{typ}})=d$ of the multifractal spectrum $f(\alpha)$ introduced in Eq. (1). (Note that in Refs. 9 and 10), κ_{typ} is denoted by X_t and α_{typ} by α_0. Here we have chosen to use the explicit notation "typ" for clarity).

For the PRBM considered here, the dimension is $d=1$ and critical exponents depend continuously on b. We show on Fig. 2(a) the $\ln T_L^{\text{typ}}$ as a function of $\ln L$: the slopes allow us to measure the exponents $\kappa_{\text{typ}}(b)$

$$\ln T_L^{\text{typ}}(a=1,b) \equiv \overline{\ln T_L(a=1,b)} \underset{L\to\infty}{\propto} -\kappa_{\text{typ}}(b)\ln L. \tag{22}$$

On Fig. 2(b), we show how the exponent $\kappa_{\text{typ}}(b)$ depends on b. The values $\kappa_{\text{typ}}(b)$ we have measured are listed in Table I,

TABLE I. Critical exponents as a function of b: (i) the exponent $\kappa_{\rm typ}(b)$ characterizes the typical transmission at criticality [see Eq. (22)], (ii) the corresponding value of the typical exponent $\alpha_{\rm typ}=1+\kappa_{\rm typ}(b)/2$ [see Eq. (20)] for the weight $\psi^2(\vec{r})$ of eigenfunctions [see Eq. (21)].

b	$b\to 0$	0.01	0.05	0.1	0.25	0.5	1	4	10	$b\to+\infty$
$\kappa_{\rm typ}(b)$	2	1.92	1.64	1.33	0.77	0.46	0.25	0.08	0.04	0
$\alpha_{\rm typ}(b)=1+\frac{\kappa_{\rm typ}(b)}{2}$	2	1.96	1.82	1.66	1.38	1.23	1.12	1.04	1.02	1

together with the corresponding values of $\alpha_{\rm typ}(b)$ obtained via Eq. (20): these values of $\alpha_{\rm typ}(b)$ are compatible with the values of the maxima of the multifractal spectrum $f(\alpha)$ of critical eigenstates measured in Ref. 15 (see Figs. 2 and 6 of Ref. 15) and in Ref. 20 (see Figs. 2 and 3 of Ref. 20).

The two limits $b\gg 1$ and $b\ll 1$ can be understood as follows. The case $b\gg 1$ corresponds to very weak multifractality with the typical exponent $\alpha_{\rm typ}\to 1$.[15,20] Equation (20) yields that the critical exponent $\kappa_{\rm typ}$ of the typical transmission becomes arbitrary small in the limit $b\to+\infty$,

$$\kappa_{\rm typ}(b\to+\infty)\to 0. \tag{23}$$

The opposite limit $b\ll 1$ corresponds to very strong multifractality with the typical exponent $\alpha_{\rm typ}\to 2$.[15,20] Equation (20) thus yields

$$\kappa_{\rm typ}(b\to 0)\to 2. \tag{24}$$

B. Multifractal spectrum $\Phi_b(\kappa)$ with termination at $\kappa=0$

As recalled in Sec. I, the statistics of the two-point transmission is expected to be multifractal at criticality, as a consequence of the multifractal character of critical eigenfunctions.[9] For the PRBM, the multifractal spectrum $\Phi_b(\kappa)$ of Eq. (7) will depend continuously on the parameter b

$$\mathrm{Prob}(T_L\sim L^{-\kappa})dT \underset{L\to\infty}{\propto} L^{\Phi_b(\kappa)}d\kappa. \tag{25}$$

Since it describes a probability, the multifractal spectrum satisfies $\Phi_b(\kappa)\leq 0$, and the maximal value $\Phi_b(\kappa)=0$ is reached only for the typical value $\kappa=\kappa_{\rm typ}(b)$ as discussed above

$$\Phi_b[\kappa_{\rm typ}(b)]=0. \tag{26}$$

The relation of Eq. (20) between the two typical exponents $\kappa_{\rm typ}(b)$ and $\alpha_{\rm typ}(b)$ is expected to come from the more general relation of Eq. (11) between the two multifractal spectra $\Phi_b(\kappa)$ and $f_b(\alpha)$,

$$\Phi_b(\kappa\geq 0)=2\left[f_b\left(\alpha=1+\frac{\kappa}{2}\right)-1\right]. \tag{27}$$

An essential property of the spectrum $\Phi_b(\kappa)$ is that it exists only for $\kappa\geq 0$ as a consequence of the physical bound $T_L\leq 1$ so that it terminates at $\kappa=0$ at the finite value

$$\Phi_b(\kappa=0)=2[f_b(\alpha=1)-1]. \tag{28}$$

To measure numerically the multifractal spectrum $\Phi_b(\kappa)$, we have used the standard method based on q measures of Ref. 35 (see more details in Appendix B). To show how the parameter b allows us to interpolate between weak multifractality and strong multifractality, we compare on Fig. 3(a) the multifractal spectra $\Phi_b(\kappa)$ for the three values $b=1$, $b=0.1$, and $b=0.01$. For instance, for the value $b=0.1$, the termination value we measure $\Phi_b(\kappa=0)\sim -0.58$ is in agreement via Eq. (28) with the value $f_b(\alpha=1)\sim 0.71$ of Fig. 6 of Ref. 15 and Fig. 2 of Ref. 20.

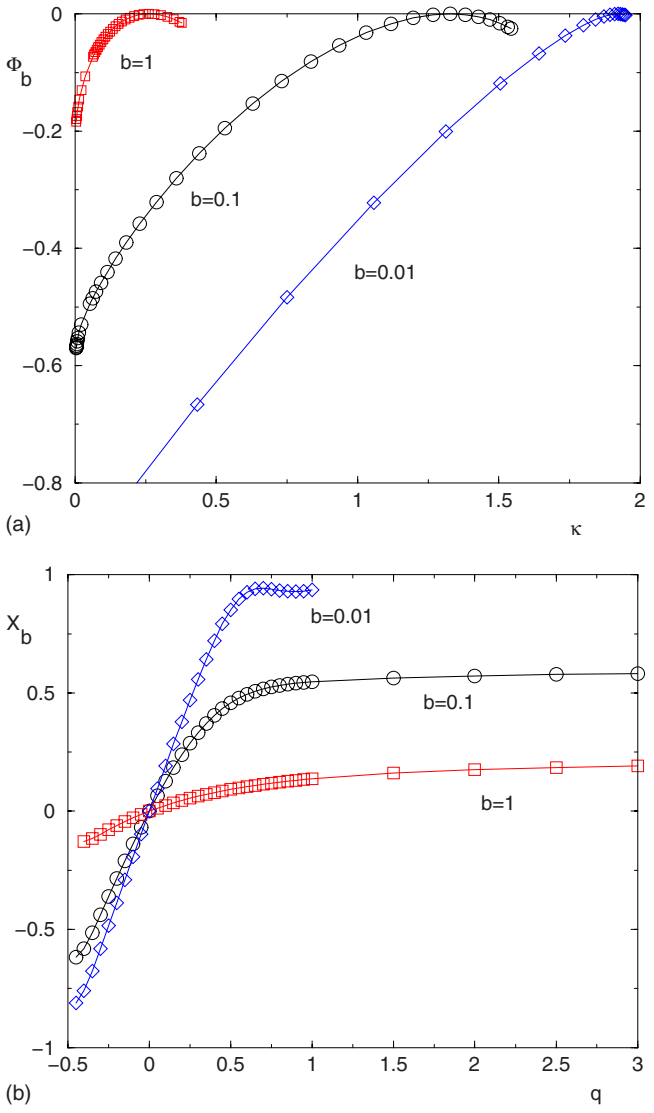

FIG. 3. (Color online) Multifractal statistics of the critical two-point transmission for three values $b=1$, $b=0.1$, and $b=0.01$: (a) the multifractal spectra $\Phi_b(\kappa)$ reach their maximum $\Phi_b[\kappa_{\rm typ}(b)]=0$ at the typical values $\kappa_{\rm typ}(b)$ and exactly terminate at finite values $\Phi_b(\kappa=0)$. (b) the corresponding moments exponents $X_b(q)$ become completely frozen for $q\geq q_{\rm sat}$: $X_b(q\geq q_{\rm sat})=-\Phi_b(\kappa=0)$.

C. Freezing transition of the moments exponents $X_b(q)$

As usual, the multifractal statistics of Eq. (25) has for consequence that the moments of arbitrary order q,

$$\overline{T_L^q} \sim \int d\kappa L^{\Phi_b(\kappa)-q\kappa} \underset{L\to\infty}{\propto} L^{-X_b(q)}, \tag{29}$$

are governed by nontrivial exponents $X_b(q)$ that can be obtained via the saddle-point calculation

$$-X_b(q) = \max_{\kappa\geq 0}[\Phi_b(\kappa) - \kappa q]. \tag{30}$$

As long as the saddle-point value satisfies $\kappa(q)\geq 0$, $X_b(q)$ can be obtained via the usual Legendre transform formula

$$q = \Phi_b'(\kappa),$$

$$X_b(q) = \kappa q - \Phi_b(\kappa). \tag{31}$$

However above some threshold $q_{\rm sat}$, the saddle-point value will saturate to the boundary value

$$\kappa(q \geq q_{\rm sat}) = 0 \tag{32}$$

and the exponent $X(q)$ will saturate to the value

$$X_b(q \geq q_{\rm sat}) = X_b(q_{\rm sat}) = -\Phi_b(\kappa = 0) = 2[1 - f_b(\alpha = 1)]. \tag{33}$$

This freezing phenomenon of $X(q)$ at $q_{\rm sat}$ predicted in Ref. 9 means that all moments of order $q\geq q_{\rm sat}$ are dominated by the rare events corresponding to a finite transmission $T\simeq 1$ whose measure behaves as $L^{\Phi(\kappa=0)}$.

We show on Fig. 3(a) the moments exponents $X_b(q)$ for the three values $b=1$, $b=0.1$, and $b=0.01$. For instance for $b=0.1$, the freezing value $X_b(q\geq q_{\rm sat})\sim 0.58$ corresponds to the termination value $\Phi_b(\kappa=0)\sim -0.58$ of Fig. 3(a).

It turns out that for Anderson transitions, a special symmetry of the multifractal spectrum $f(\alpha)$ has been proposed (see Refs. 20 and 36 and references therein) that relates the regions $\alpha\leq d$ and $\alpha\geq d$ via the relation $f(2d-\alpha)=f(\alpha)+d-\alpha$. This symmetry then fixes the value of $q_{\rm sat}$ where $\kappa(q_{\rm sat})=0$ or equivalently $\alpha(q_{\rm sat})=d$ to be exactly

$$q_{\rm sat} = \frac{1}{2}. \tag{34}$$

Numerically, it is difficult to measure precisely the value $q_{\rm sat}$ where the exponents $X_b(q)$ become completely frozen as a consequence of finite-size corrections around this phase-transition point for the $X(q)$, as already found for the quantum-Hall transition in Ref. 9 However Fig. 3(b) shows that in the limit of strong multifractality ($b=0.01$), the numerical saturation value is not far from the theoretical prediction of Eq. (34).

IV. STATISTICS OF THE TWO-POINT TRANSMISSION IN THE LOCALIZED PHASE ($a>1$)

A. Typical transmission in the localized phase

In usual short-range models, the localized phase is characterized by exponentially localized wave functions, whereas in the presence of power-law hoppings, localized wave function can only decay with power-law integrable tails. For the PRBM, it is moreover expected that the asymptotic decay is actually given exactly by the power law of Eq. (13) for the hopping term defining the model:[11] $|\psi(r)|^2_{\rm typ}\sim 1/r^{2a}$. As a consequence in the localized phase $a>1$, one expects the typical decay

$$T_L^{\rm typ}(a>1) \underset{L\to\infty}{\propto} \frac{1}{L^{2a}}. \tag{35}$$

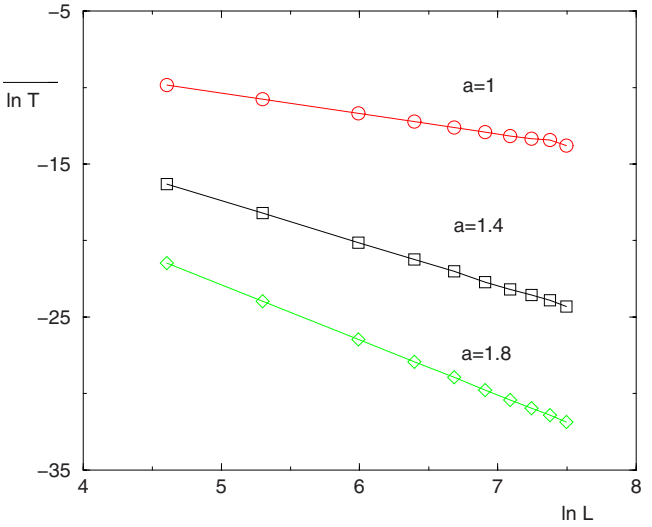

FIG. 4. (Color online) Typical two-point transmission in the localized phase $a>1$. The power-law decay of Eq. (35) is checked here for the case $b=0.1$ and the two values $a=1.4$ and $a=1.8$: the slopes of this log-log plot are of order $2a\sim 2.8$ and $2a\sim 3.6$. For comparison, we also show the critical data for $a=1$ of slope $\kappa_{\rm typ}(b=0.1)\sim 1.33$.

As shown on Fig. 4, we have checked this power-law decay of the typical transmission for the case $b=0.1$ and the two values $a=1.4$ and $a=1.8$.

B. Histogram of ($\ln T_L$) in the localized phase ($a>1$)

We show on Fig. 5 the histograms P_L of $\ln T_L$ for the four sizes $L=100,200,400,800$ in the localized phase $a=1.4$ for the case $b=0.1$: these data seem to indicate that as L grows, the probability distribution shifts to the left while keeping a fixed shape. This means that the relative variable $u=(\ln T_L - \ln T_L^{\rm typ})$ with respect to the typical value discussed above [see Eq. (35)] remains a finite variable as $L\to+\infty$. In addition, the left tail is governed by the exponent $\alpha\sim 0.5$

$$\ln P_\infty^{\rm loc}[u = (\ln T_L - \ln T_L^{\rm typ})] \underset{u\to-\infty}{\simeq} \frac{1}{2}u \tag{36}$$

or equivalently after the change in variable $\mathcal{T}=\frac{T_L}{T_L^{\rm typ}}=e^u$

$$P_\infty^{\rm loc}\left(\mathcal{T} = \frac{T_L}{T_L^{\rm typ}}\right) \underset{\mathcal{T}\to 0}{\propto} \frac{1}{\mathcal{T}^{1/2}}. \tag{37}$$

These properties can be understood by the following simple argument. In the localized phase $a>1$, one may as-

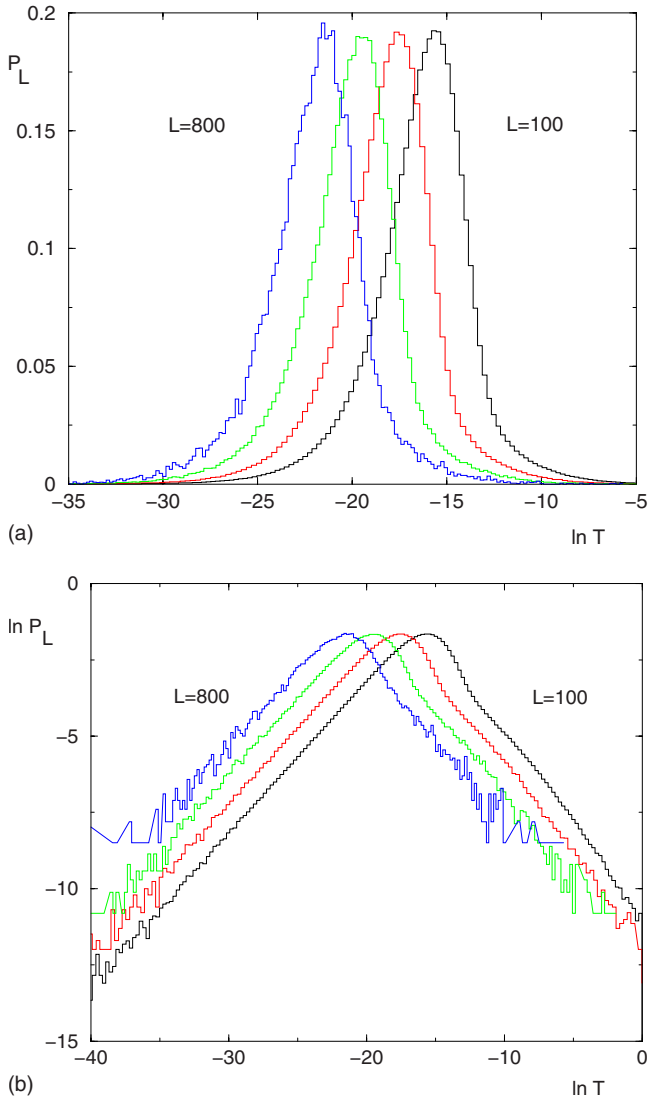

FIG. 5. (Color online) Histogram of of the two-point transmission in the localized phase $a>1$: example for $b=0.1$ and $a=1.4$: (a) histograms P_L of $\ln T_L$ for the four sizes $L=100,200,400,800$ (the histograms for bigger sizes are more noisy and are not shown for clarity) (b) same data in logarithmic scale to exhibit the tails discussed in the text.

sume that for large L, the transmission T_L is dominated by the direct hopping term $H_{L/2,L}$ (see Fig. 1),

$$T_L(a>1) \underset{L\to\infty}{\propto} |H_{L/2,L}|^2 \underset{L\to\infty}{\propto} \frac{x^2}{L^{2a}}, \tag{38}$$

where x is a Gaussian variable of zero mean and variance unity [see Eq. (13)]. In particular, its probability density is finite near the origin $P(x=0)>0$. The change in variable

$$\mathcal{T} = \frac{T_L}{T_L^{\rm typ}} \propto x^2 \tag{39}$$

then yields the power law of Eq. (37).

V. STATISTICS OF THE TWO-POINT TRANSMISSION IN THE DELOCALIZED PHASE ($a<1$)

A. Typical transmission in the delocalized phase

In the delocalized phase, the eigenfunctions are not multifractal anymore but monofractal with the single value $\alpha_{\rm deloc}=d$ for the weight As a consequence, the typical transmission is expected to remain finite as $L\to+\infty$ (Ref. 9) [in Eq. (20), the case $\alpha_{\rm typ}=d$ yields $\kappa_{\rm typ}=0$]

$$T_L^{\rm typ} \underset{L\to\infty}{\propto} T_\infty^{\rm typ} > 0. \tag{40}$$

The two-point transmission is thus a good order parameter of the transport properties.[9]

B. Histogram of ($\ln T_L$) in the delocalized phase $a<1$

We find that the whole probability distribution $P_L(\ln T)$ converges for large L toward a fixed distribution $P_\infty^{\rm deloc}(\ln T)$. As an example, we show on Fig. 6 the histograms of ($\ln T_L$) for three sizes $L=100,200,400$ concerning the case $b=1$ and $a=0.75$. These histograms stops at $\ln T=0$ as a consequence of the bound $T\leq 1$. In the region of very small transmission $\ln T\to-\infty$ the log-log plot of Fig. 6(b) indicates the same form as in Eq. (36)

$$\ln P_\infty^{\rm deloc}(\ln T) \underset{\ln T\to-\infty}{\propto} \frac{1}{2}\ln T \tag{41}$$

or equivalently after a change in variable

$$P_\infty^{\rm deloc}(T) \underset{T\to 0}{\propto} \frac{1}{T^{1/2}}. \tag{42}$$

As explained around Eq. (39), this power-law behavior simply means that the transmission can be written as the square $T\simeq x^2$ of some random variable x that has a finite probability density at the origin $P(x=0)>0$. This means that all negative moments of order $q\leq -1/2$ actually diverge in the delocalized phase

$$\int_0^1 dT T^q P_\infty^{\rm deloc}(T) \underset{q\leq -1/2}{\simeq} +\infty. \tag{43}$$

VI. CONCLUSIONS AND PERSPECTIVES

In this paper, we have studied numerically the statistics of the two-point transmission T_L as a function of the size L in the PRBM model that depends on two parameters (a,b): (i) in the delocalized phase ($a<1$), we have found that the probability distribution of T_L converges for $L\to+\infty$ toward a law $P_\infty^{\rm deloc}(T)$ presenting the power law of Eq. (42) for $T\to 0$. (ii) in the localized phase ($a>1$), we have found that the probability distribution $P_L^{\rm loc}(\ln T_L)$ keeps a fixed shape around the typical value $\ln T^{\rm typ}=\ln T_L$ as L grows and the typical value $T_L^{\rm typ}$ decays only as the power law of Eq. (35) as a consequence of the presence of power-law hoppings. (iii) exactly at criticality ($a=1$), the statistics of the two-point transmission T_L is multifractal: we have measured the multifractal spectra $\Phi_b(\kappa)$ as well as the moments exponents

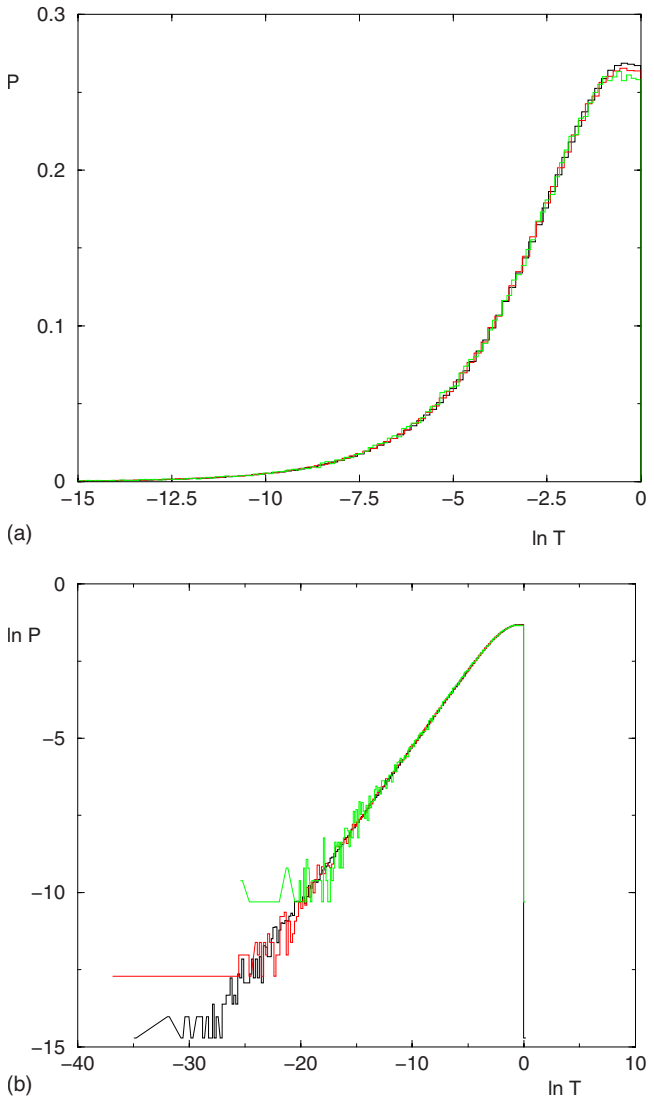

FIG. 6. (Color online) Histogram of of the two-point transmission in the delocalized phase $a<1$: example for $b=1$ and $a=0.75$ (a) the histograms of $\ln T_L$ for the three sizes $L=100,200,400$ coincide (the histograms for bigger sizes are more noisy and are not shown for clarity) (b) same data in logarithmic scale to exhibit the tail [see Eq. (41)].

$X_b(q)$ for various values of the parameter b that allows us to interpolate between weak multifractality and strong multifractality. We have tested in detail the various expectations of Ref. 9 concerning the termination of $\Phi_b(\kappa)$ at $\kappa=0$, the freezing of $X_b(q)$ above some value $q \geq q_{\rm sat}$, and the relations with the singularity spectrum $f_b(\alpha)$ of individual critical eigenstates. To finish, we should stress that the relation of Eq. (11) relates the transmission between two "bulk points" to the "bulk multifractal spectrum" $f(\alpha)$. In localization models, it is however more usual to attach leads to the boundaries of the disordered sample: then the statistics of the two-point transmission is related to the "surface multifractal spectrum" as will be discussed in more details elsewhere.[37] We will also discuss in Ref. 37 the statistical properties of the transmission for various scattering geometries involving a large number of wires.

APPENDIX A: COMPUTATION OF THE TWO-POINT TRANSMISSION IN EACH SAMPLE

To compute the transmission of a given sample via Eq. (16), we have to solve the Schödinger problem of Eq. (14) with the scattering boundary conditions of Eq. (15). This can be decomposed in two steps as follows.

1. Recursive elimination of the "interior sites"

The first step consists in the iterative elimination of the interior sites, i.e., of all the sites not connected to the external wires (see Fig. 1). To eliminate the site i_0, one uses the Schödinger Eq. (14) projected on this site

$$E\psi(i_0) = H_{i_0,i_0}\psi(i_0) + \sum_j H_{i_0,j}\psi(j) \tag{A1}$$

to make the substitution

$$\psi(i_0) = \frac{1}{E - H_{i_0,i_0}} \sum_j H_{i_0,j}\psi(j) \tag{A2}$$

in all other remaining equations. Then from the point of view of remaining sites, the hoppings are renormalized according to

$$H_{i,j}^{\rm new} = H_{i,j} + \frac{H_{i,i_0}H_{i_0,j}}{E - H_{i_0,i_0}}. \tag{A3}$$

This procedure is stopped when the only remaining sites are the two sites $L/2$ and L connected to the external wires (see Fig. 1): the three real remaining parameters are the renormalized hopping $\tilde{H}_{L/2,L}$ and the two renormalized on-site energies $\tilde{H}_{L/2,L/2}$ and $\tilde{H}_{L,L}$.

2. Effective scattering problems for the two boundary sites

The second step consists in solving the scattering problem for the two boundary sites $L/2$ and L connected to the external wires (see Fig. 1) with the renormalized parameters obtained above. The Schödinger Eq. (14) projected on the boundary sites $L/2$ and L read

$$E\psi(x_{L/2}) = \tilde{H}_{L/2,L/2}\psi(x_{L/2}) + \psi(x_{L/2}-1) + \tilde{H}_{L/2,L}\psi(x_L),$$

$$E\psi(x_L) = \tilde{H}_{L,L}\psi(x_L) + \psi(x_L+1) + \tilde{H}_{L,L/2}\psi(x_{L/2}). \tag{A4}$$

The boundary conditions of Eq. (15) fixes the following ratio on the outgoing wire:

$$\frac{\psi(x_L+1)}{\psi(x_L)} = e^{ik}. \tag{A5}$$

The following ratio:

$$R \equiv \frac{\psi(x_{L/2}-1)}{\psi(x_{L/2})}, \tag{A6}$$

concerning the incoming wire can be then computed in terms of the three real-renormalized parameters,

$$R = E - \tilde{H}_{L/2,L/2} - \frac{\tilde{H}^2_{L,L/2}}{E-(\tilde{H}_{L,L}+e^{ik})}. \tag{A7}$$

The reflexion coefficient r of Eq. (15) is then obtained as

$$r = \frac{R-e^{-ik}}{e^{ik}-R}, \tag{A8}$$

yielding the transmission of Eq. (16).

APPENDIX B: COMPUTATION OF THE MULTIFRACTAL SPECTRUM OVER THE SAMPLES

To measure numerically the multifractal spectrum $\Phi(\kappa)$ of Eq. (7) that characterizes the statistics of the transmission T_L over the samples of size L, we have used the standard method based on q measures of Ref. 35. More precisely, for various sizes L, we have measured the transmission $T_L(i)$ for a number $n_s(L)$ of independent samples (i). Then for various values of q, we have computed the moments of Eq. (8)

$$\overline{T_L^q} = \frac{1}{n_s(L)} \sum_{i=1}^{n_s(L)} [T_L(i)]^q \tag{B1}$$

to extract the moments exponents $X(q)$ as the slope of the log-log plot

$$\ln(\overline{T_L^q}) \underset{L\to\infty}{\propto} -X(q)\ln L. \tag{B2}$$

We have also computed the auxiliary observables

$$K_L(q) = \frac{\sum_{i=1}^{n_s(L)} [T_L(i)]^q [-\ln T_L(i)]}{\sum_{i=1}^{n_s(L)} [T_L(i)]^q} \tag{B3}$$

and

$$F_L(q) = qK_L(q) + \ln(\overline{T_L^q}) \tag{B4}$$

to obtain $\kappa(q)$ and $\Phi[\kappa(q)]$ as the slopes of

$$K_L(q) \underset{L\to\infty}{\propto} \kappa(q)\ln L \tag{B5}$$

and

$$F_L(q) \underset{L\to\infty}{\propto} \Phi[\kappa(q)]\ln L \tag{B6}$$

This yields a parametric plot in q of the multifractal spectrum $\Phi(\kappa)$: on Fig. 3(a), each circle of coordinate $[\kappa,\Phi(\kappa)]$ corresponds to a value of q.

[1] P. W. Anderson, Phys. Rev. **109**, 1492 (1958).
[2] D. J. Thouless, Phys. Rep. **13**, 93 (1974); D. J. Thouless, in *Condensed Matter*, edited by R. Balian, R. Maynard, and G. Toulouse (North-Holland, Amsterdam, 1979).
[3] B. Souillard, in *Chance and Matter*, edited by J. Souletie, J. Vannimenus, and R. Stora (North-Holland, Amsterdam, 1987).
[4] I. M. Lifshitz, S. A. Gredeskul, and L. A. Pastur, *Introduction to the Theory of Disordered Systems* (Wiley, New York, 1988).
[5] B. Kramer and A. MacKinnon, Rep. Prog. Phys. **56**, 1469 (1993).
[6] M. Janssen, Phys. Rep. **295**, 1 (1998).
[7] P. Markos, Acta Phys. Slov. **56**, 561 (2006).
[8] F. Evers and A. D. Mirlin, Rev. Mod. Phys. **80**, 1355 (2008).
[9] M. Janssen, M. Metzler, and M. R. Zirnbauer, Phys. Rev. B **59**, 15836 (1999).
[10] F. Evers, A. Mildenberger, and A. D. Mirlin, Phys. Status Solidi **245**, 284 (2008).
[11] A. D. Mirlin, Y. V. Fyodorov, F. M. Dittes, J. Quezada, and T. H. Seligman, Phys. Rev. E **54**, 3221 (1996).
[12] I. Varga and D. Braun, Phys. Rev. B **61**, R11859 (2000).
[13] V. E. Kravtsov, O. Yevtushenko, and E. Cuevas, J. Phys. A **39**, 2021 (2006).
[14] A. M. Garcia-Garcia, Phys. Rev. E **73**, 026213 (2006).
[15] F. Evers and A. D. Mirlin Phys. Rev. Lett. **84**, 3690 (2000); A. D. Mirlin and F. Evers, Phys. Rev. B **62**, 7920 (2000).
[16] E. Cuevas, V. Gasparian, and M. Ortuno, Phys. Rev. Lett. **87**, 056601 (2001).
[17] E. Cuevas, M. Ortuno, V. Gasparian, and A. Perez-Garrido, Phys. Rev. Lett. **88**, 016401 (2001).
[18] I. Varga, Phys. Rev. B **66**, 094201 (2002).
[19] E. Cuevas, Phys. Rev. B **68**, 024206 (2003).
[20] A. D. Mirlin, Y. V. Fyodorov, A. Mildenberger, and F. Evers, Phys. Rev. Lett. **97**, 046803 (2006).
[21] A. Mildenberger, A. R. Subramaniam, R. Narayanan, F. Evers, I. A. Gruzberg, and A. D. Mirlin, Phys. Rev. B **75**, 094204 (2007).
[22] J. A. Mendez-Bermudez and T. Kottos, Phys. Rev. B **72**, 064108 (2005).
[23] J. A. Mendez-Bermudez and I. Varga, Phys. Rev. B **74**, 125114 (2006).
[24] R. P. A. Lima, F. A. B. F. de Moura, M. L. Lyra, and H. N. Nazareno, Phys. Rev. B **71**, 235112 (2005).
[25] R. P. A. Lima, H. R. da Cruz, J. C. Cressoni, and M. L. Lyra, Phys. Rev. B **69**, 165117 (2004).
[26] H. Potempa and L. Schweitzer, Phys. Rev. B **65**, 201105(R) (2002).
[27] E. Cuevas, Phys. Status Solidi **241**, 2109 (2004).
[28] E. Cuevas, Phys. Rev. B **71**, 024205 (2005).
[29] L. S. Levitov, Europhys. Lett. **9**, 83 (1989); Phys. Rev. Lett. **64**, 547 (1990); B. L. Altshuler and L. S. Levitov, Phys. Rep. **288**, 487 (1997); L. S. Levitov, Ann. Phys. **8**, 507 (1999).
[30] R. Landauer, Philos. Mag. **21**, 863 (1970).
[31] P. W. Anderson, D. J. Thouless, E. Abrahams, and D. S. Fisher,

Phys. Rev. B **22**, 3519 (1980).
[32] P. W. Anderson and P. A. Lee, Suppl. Prog. Theor. Phys. **69**, 212 (1980).
[33] J. M. Luck, *Systèmes Désordonnés Unidimensionnels* (Alea Saclay, Gif-sur-Yvette, France, 1992).
[34] A. D. Stone and A. Szafer, IBM J. Res. Dev. **32**, 384 (1988).
[35] A. Chhabra and R. V. Jensen, Phys. Rev. Lett. **62**, 1327 (1989).
[36] L. J. Vasquez, A. Rodriguez, and R. A. Romer, Phys. Rev. B **78**, 195106 (2008); A. Rodriguez, L. J. Vasquez, and R. A. Romer, *ibid.* **78**, 195107 (2008); A. Rodriguez, L. J. Vasquez, and R. A. Romer, Phys. Rev. Lett. **102**, 106406 (2009).
[37] C. Monthus and T. Garel, arXiv:0904.4547 (unpublished).